Forecasting the Cosmological Constraints with Anisotropic Baryon Acoustic Oscillations from Multipole Expansion

Atsushi Taruya[1,2], Shun Saito[3,4], Takahiro Nishimichi[2]
[1]*Research Center for the Early Universe, School of Science, The University of Tokyo, Bunkyo-ku, Tokyo 113-0033, Japan*
[2]*Institute for the Physics and Mathematics of the Universe, The University of Tokyo, Kashiwa, Chiba 277-8568, Japan*
[3]*Department of Physics, The University of Tokyo, 113-0033, Japan and*
[4]*Department of Astronomy, University of California Berkley, California 94720, USA*
(Dated: January 26, 2011)

Baryon acoustic oscillations (BAOs) imprinted in the galaxy power spectrum can be used as a standard ruler to determine angular diameter distance and Hubble parameter at high redshift galaxies. Combining redshift distortion effect which apparently distorts the galaxy clustering pattern, we can also constrain the growth rate of large-scale structure formation. Usually, future forecast for constraining these parameters from galaxy redshift surveys has been made with a full 2D power spectrum characterized as function of wavenumber k and directional cosine μ between line-of-sight direction and wave vector, i.e., $P(k,\mu)$. Here, we apply the multipole expansion to the full 2D power spectrum, and discuss how much cosmological information can be extracted from the lower-multipole spectra, taking a proper account of the non-linear effects on gravitational clustering and redshift distortion. The Fisher matrix analysis reveals that compared to the analysis with full 2D spectrum, a partial information from the monopole and quadrupole spectra generally degrades the constraints by a factor of ~ 1.3 for each parameter. The additional information from the hexadecapole spectrum helps to improve the constraints, which lead to an almost comparable result expected from the full 2D spectrum.

I. INTRODUCTION

Baryon acoustic oscillations (BAOs) imprinted on the clustering of galaxies are now recognized as a powerful cosmological probe to trace the expansion history of the Universe [1–3]. In particular, the BAO measurement via a spectroscopic survey can provide a way to simultaneously determine the angular diameter distance D_A and Hubble parameter H at given redshift of galaxies through the cosmological distortion, known as Alcock-Paczynski effect (e.g., [4–8]). Further, measuring the clustering anisotropies caused by the redshift distortion due to the peculiar velocity of galaxies, we can also probe the growth history of structure formation (e.g., [9–12]), characterized by the growth-rate parameter $f \equiv d\ln D/d\ln a$, with quantities D and a being linear growth factor and the scale factor of the Universe, respectively.

With the increased number of galaxies and large survey volumes, on-going and future spectroscopic galaxy surveys such as Baryon Oscillation Spectroscopic Survey (BOSS) [13], Hobby-Eberly Dark Energy Experiment (HETDEX) [14], Subaru Measurement of Imaging and Redshift equipped with Prime Focus Spectrograph (SuMIRe-PFS), and EUCLID/JDEM [15, 16] aim at precisely measuring the acoustic scale of BAOs as a standard ruler. These surveys will cover the wide redshift ranges, $0.3 \lesssim z \lesssim 3.5$, and provide a precision data of the redshift-space power spectrum with an accuracy of a percent level over the scales of BAOs.

In promoting these gigantic surveys, a crucial task is a quantitative forecast for the size of the statistical errors on the parameters D_A, H and f in order to clarify the scientific benefits as well as to explore the optimal survey design. The Fisher matrix formalism is a powerful tool to investigate these issues, and it enables us to quantify the precision and the correlation between multiple parameters ([5, 7, 17, 18], especially for measuring D_A, H and f). So far, most of the works on the parameter forecast study have focused on the potential power of the BAO measurements, and attempt to clarify the achievable level of the precision for the parameter estimation. For this purpose, they sometimes assumed a rather optimistic situation that a full shape of the redshift-space power spectrum, including the clustering anisotropies due to the redshift distortion, is available in both observation and theory.

In this paper, we are particularly concerned with the parameter estimation using a partial information of the anisotropic BAOs from a practical point-of-view. In redshift space, the power spectrum obtained from the spectroscopic measurement is generally described in the two dimension, and is characterized as functions of k and μ, where k is the wavenumber and μ is the directional cosine between the line-of-sight direction and k [49]. While most of the forecast study is concerned with a full 2D power spectrum, the multipole expansion of redshift-space power spectrum has been frequently used in the data analysis to quantify the clustering anisotropies. Denoting the power spectrum by $P(k,\mu)$, we have

$$P(k,\mu) = \sum_{\ell=0}^{\text{even}} P_\ell(k)\,\mathcal{P}_\ell(\mu) \tag{1}$$

with the function $\mathcal{P}_\ell$ being the Legendre polynomials. Although the analysis with full 2D spectrum will definitely

play an important role as improving the statistical signal, most of the recent cosmological data analysis has focused on the angle-averaged power spectrum ($\ell = 0$), i.e., monopole spectrum, and a rigorous analysis with full 2D spectrum is still heavy task due to the time-consuming covariance estimation (e.g., [19–21]).

In linear theory, the redshift-space power spectrum is simply written as $P(k,\mu) = (1+\beta\,\mu^2)^2 P_{\rm gal}(k)$, where $\beta = f/b$ with b being the linear bias parameter, and $P_{\rm gal}$ is the galaxy power spectrum in real space [22–24]. Then, the non-vanishing components arises only from the monopole ($\ell = 0$), quadrupole ($\ell = 2$) and hexadecapole spectra ($\ell = 4$). That is, cosmological information contained in the $\ell = 0$, 2 and 4 moments is equivalent to the whole information in the full 2D power spectrum. Observationally, however, this is only the case when we a priori know the cosmological distance to the galaxies. The Alcock-Paczynski effect can induce non-trivial clustering anisotropies, which cannot be fully characterized by the lower multipole spectra, in general. Further, in reality, linear theory description cannot be adequate over the scale of the BAOs, and the non-linear effects of the redshift distortion as well as the gravitational clustering must be accounted for a proper comparison with observation. These facts imply that non-vanishing multipole spectra higher than $\ell > 4$ generically appear, and a part of the cosmological information might be leaked into those higher multipole moments. An important question is how much amount of the cosmological information can be robustly extracted from the lower multipole spectra instead of the full 2D spectrum. In the light of this, Ref. [8] recently examined a non-parametric method to constrain D_A and H from the monopole and quadrupole spectra, and numerically estimate the size of errors (see also Ref. [25] for the estimation of growth-rate parameter).

Here, as a complementary and comprehensive approach, we will investigate this issue based on the Fisher matrix formalism, and derive the useful formulae for parameter forecast using the multipole power spectra. We then explore the potential power of the lower multipole spectra on the cosmological constraints, particularly focusing on the parameters D_A, H and f. To do so, we consider the Figure-of-Merit (FoM) and Figure-of-Bias (FoB) for these parameters, and investigate their dependence on the assumptions for the number density of galaxies, the amplitude of clustering bias, the maximum wavenumber used for the parameter estimation.

In Sec. II, we present the Fisher matrix formalism for cosmological parameter estimation from the multipole power spectra. Sec. III deals with the model of redshift-space power spectrum and the assumptions used in the Fisher matrix analysis. Then, in Sec. IV, the results for FoM and FoB are shown, and the sensitivity of the results to the assumptions and choice of the parameters is discussed in greater details. Finally, Sec. V briefly summarize our present work.

Throughout the paper, we assume a flat Lambda cold dark matter (CDM) model, and the fiducial model parameters are chosen based on the five-year WMAP results [26]: $\Omega_{\rm m} = 0.279$, $\Omega_\Lambda = 0.721$, $\Omega_{\rm b} = 0.0461$, $h = 0.701$, $n_s = 0.96$, $A_s = 2.19\times10^{-9}$.

II. FISHER MATRIX FORMALISM

In this section, we present the basic formulae for Fisher matrix analysis in estimating the statistical error and systematic biases for cosmological parameters from the multipole power spectra.

Let us first derive the expression for Fisher matrix relevant for the power spectrum analysis. The definition of the Fisher matrix is given by

$$F_{ij} = -\left\langle \frac{\partial^2 \ln\mathcal{L}}{\partial\theta_i\partial\theta_j}\right\rangle, \tag{2}$$

where θ_i denotes the parameter, and the quantity $\mathcal{L}$ is the likelihood function. For the parameter estimation study with the multipole spectrum, $P_\ell(k)$, the likelihood function is usually taken in the form as

$$\mathcal{L} \propto \exp\left[-\frac{1}{2}\sum_{m,n}\sum_{\ell,\ell'}\Delta P_\ell(k_m)\left[C^{\ell\ell'}(k_m,k_n)\right]^{-1}\Delta P_{\ell'}(k_n)\right], \tag{3}$$

where we define

$$\begin{aligned}\Delta P_\ell(k) &\equiv \widehat{P}_\ell(k) - P_\ell(k),\\ C^{\ell\ell'}(k_m,k_n) &\equiv \langle \Delta P_\ell(k_m)\,\Delta P_{\ell'}(k_n)\rangle.\end{aligned}$$

The quantities $\widehat{P}_\ell(k)$ and $P_\ell(k)$ respectively denote the observed estimate and theoretical template for the multipole power spectrum.

Substituting Eq. (3) into the definition (2), the leading-order evaluation of the Fisher matrix leads to (e.g., [27, 28]):

$$F_{ij} \simeq \sum_n\sum_{\ell,\ell'}\frac{\partial P_\ell(k_n)}{\partial\theta_i}\left[{\rm Cov}^{\ell\ell'}(k_n)\right]^{-1}\frac{\partial P_\ell(k_n)}{\partial\theta_j}, \tag{4}$$

where we have assumed that the covariance is approximately characterized by the Gaussian statistic, and is written as $C^{\ell\ell'}(k_m,k_n) = {\rm Cov}^{\ell\ell'}(k_n)\,\delta_{mn}$.

Adopting the power spectrum estimation by Ref. [29], the analytic expression for the quantity ${\rm Cov}^{\ell\ell'}(k_n)$ can be found in Ref. [30] [see Eq. (25) of their paper]:

$$\begin{aligned}{\rm Cov}^{\ell\ell'}(k_n) = \frac{2}{V_n}\,\frac{(2\ell+1)(2\ell'+1)}{2}\\ \times\int_{-1}^{1}d\mu\frac{\mathcal{P}_\ell(\mu)\mathcal{P}_{\ell'}(\mu)}{\int d^3\boldsymbol{r}\;\overline{n}(\boldsymbol{r})^2[1+\overline{n}(\boldsymbol{r})\,P^{\rm (S)}(k_n,\mu)\,]^{-2}}\end{aligned} \tag{5}$$

with $\mathcal{P}_\ell(\mu)$ being the Legendre polynomial[50]. The quantity V_n is the volume element of the thin shell in

the Fourier space, i.e., $V_n = 4\pi^2 k_n^2 dk_n/(2\pi)^3$, which corresponds to $\Delta V_k/(2\pi)^3$ in the notation of Ref. [30].

Now, to simplify the formula, we consider the homogeneous galaxy samples, which implies $\overline{n}(\boldsymbol{r}) = \overline{n} = $ const. In this case, the denominator in the integrand of Eq. (5) is simplified as

$$\int d^3\boldsymbol{r}\ \overline{n}(\boldsymbol{r})^2[1+\overline{n}(\boldsymbol{r})\,P(k,\mu)\,]^{-2} = V_s\ \left\{P(k,\mu)+\frac{1}{\overline{n}}\right\}^{-2}, \quad (6)$$

where V_s denotes the survey volume. Then, taking the continuum limit, the expression for Fisher matrix can be recast as

$$F_{ij} = \frac{V_s}{4\pi^2}\int_{k_{\rm min}}^{k_{\rm max}} dk\,k^2\ \sum_{\ell,\ell'}\frac{\partial P_\ell(k)}{\partial\theta_i}\left[\widetilde{\rm Cov}^{\ell\ell'}(k)\right]^{-1}\frac{\partial P_\ell(k)}{\partial\theta_j}, \quad (7)$$

with the reduced covariance matrix $\widetilde{\rm Cov}^{\ell\ell'}(k)$ given by

$$\widetilde{\rm Cov}^{\ell\ell'}(k) = \frac{(2\ell+1)(2\ell'+1)}{2} \times\int_{-1}^{1} d\mu\,\mathcal{P}_\ell(\mu)\,\mathcal{P}_{\ell'}(\mu)\ \left[P(k,\,\mu)+\frac{1}{\overline{n}}\right]^2. \quad (8)$$

Here, the range of integration $[k_{\rm min}, k_{\rm max}]$ should be chosen through the survey properties and/or limitation of theoretical template, and, in particular, the minimum wave number is limited to $2\pi/V_s^{1/3}$.

Eq. (7) with (8) is the formula for the Fisher matrix used in the parameter estimation with multipole power spectra. This can be compared with the standard formula for full 2D power spectrum (e.g., [5, 7, 28]):

$$F_{ij}^{\rm (2D)} = \frac{V_s}{4\pi^2}\int_{k_{\rm min}}^{k_{\rm max}} dk k^2\int_{-1}^{1} d\mu\,\frac{\partial P(k,\mu)}{\partial\theta_i}\left\{P(k,\mu)+\frac{1}{\overline{n}}\right\}^{-2} \times\frac{\partial P(k,\mu)}{\partial\theta_j} \quad (9)$$

That is, the full 2D information obtained through the integral over directional cosine μ in Eq.(9) is replaced with the summation over all multipoles in the new formula (7). Thus, truncating the summation at a lower multipole generally leads to the reduction of the amplitude in Fisher matrix, and as a result, the statistical errors of the parameter θ_i marginalized over other parameters, given by $\Delta\theta_i = \sqrt{\{F^{-1}\}_{ii}}$, is expected to become larger.

The Fisher matrix formalism also provides a simple way to estimate the biases in the best-fit parameters caused by the incorrect template for the multipole power spectra $P_\ell^{\rm wrong}(k)$. To derive the formula for systematic bias, we replace the template power spectrum $P_\ell(k)$ in the likelihood function (3) with the incorrect one $P_\ell^{\rm wrong}(k)$. We denote this likelihood function by $\mathcal{L}'$. Assuming that the size of the biases are basically small, the (biased) best-fit values can be estimated from the extremum of the Likelihood function $\mathcal{L}'$ by expanding the expression of the extremum around the fiducial parameters:

$$0 = \frac{\partial\ln\mathcal{L}'}{\partial\theta_j} \simeq \left.\frac{\partial\ln\mathcal{L}'}{\partial\theta_j}\right|_{\rm fid} + \sum_i\left.\frac{\partial\ln\mathcal{L}'}{\partial\theta_i\partial\theta_j}\right|_{\rm fid}\delta\theta_i, \quad (10)$$

where the quantities with subscript $_{\rm fid}$ stand for the one evaluated at the fiducial parameters, and the $\delta\theta_i$ means the deviation of the best-fit value from the fiducial parameter. Then, taking the ensemble average of the above expressions and using the definition of the Fisher matrix, we obtain

$$\delta\theta_i = -\sum_j (F')^{-1}_{ij}s_j, \quad (11)$$

where the Fisher matrix F'_{ij} is the same one as given by Eq. (7), but is evaluated using incorrect power spectra $P_\ell^{\rm wrong}(k)$. The vector s_j is

$$s_j = \frac{V_s}{4\pi^2}\int_{k_{\rm min}}^{k_{\rm max}} dk\,k^2\sum_{\ell,\ell'}P_\ell^{\rm sys}(k)\left[\widetilde{\rm Cov}^{\ell\ell'}(k)\right]^{-1}\frac{\partial P_{\ell'}^{\rm wrong}(k)}{\partial\theta_j}. \quad (12)$$

Here, the multipole power spectrum $P_\ell^{\rm sys}(k)$ denotes the systematic difference between correct and incorrect model of multipole power spectra, $P_\ell^{\rm sys}(k) = P_\ell^{\rm wrong}(k) - P_\ell^{\rm true}(k)$. In deriving the above expression, we have used the fact that the extremum of the likelihood function vanishes only when the correct template for the multipole power spectrum is applied.

Notice that similar but essentially different formula for systematic biases is obtained in the cases using the full 2D power spectrum. It is formally expressed as Eq. (11), but the Fisher matrix F'_{ij} is now replaced with Eq. (9) evaluated using the incorrect 2D spectrum $P^{\rm wrong}(k,\mu)$. Further, the vector s_j should be replaced with the one for the full 2D spectrum (e.g., [31, 32]):

$$s_j^{\rm (2D)} = \frac{V_s}{4\pi^2}\int_{k_{\rm min}}^{k_{\rm max}} dk\,k^2\int_{-1}^{1} d\mu\ P^{\rm sys}(k,\mu) \times\left[P_{\ell'}^{\rm wrong}(k,\mu)+\frac{1}{\overline{n}_{\rm g}}\right]^{-2}\frac{\partial P^{\rm wrong}(k,\mu)}{\partial\theta_j}. \quad (13)$$

Finally, all the formulae derived in this section ignore the non-Gaussian contributions to the likelihood and covariances, which would be sometimes important in practice. The extension of the formulae to include the non-Gaussian contributions is straightforward, and will be considered elsewhere. For the effects of non-Gaussian contributions to the parameter estimation study especially focusing on BAOs, several works have been recently done based on the numerical and analytical treatments [20, 33, 34].

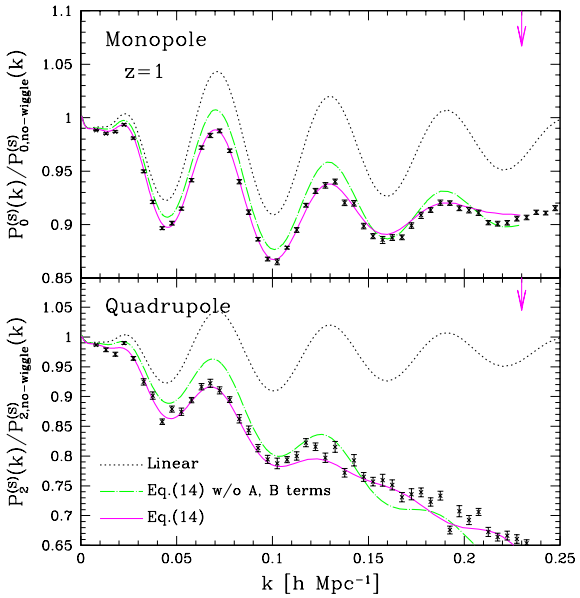

FIG. 1: Monopole (top) and quadrupole (bottom) moments of matter power spectra in redshift space at $z = 1$. The results are divided by the smooth reference spectrum, $P^{(\mathrm{S})}_{\ell,\mathrm{no\text{-}wiggle}}$, and are compared with the N-body results (symbols) taken from the `wmap5` simulations of Ref. [35]. The reference spectrum $P^{(\mathrm{S})}_{\ell,\mathrm{no\text{-}wiggle}}$ is calculated from the no-wiggle approximation of the linear transfer function [36] with the linear theory of the Kaiser effect taken into account. Solid and dot-dashed lines represent the results of improved PT calculations based on the model of redshift distortion (14), but the terms A and B are ignored in the dot-dashed lines. In both cases, the one-dimensional velocity dispersion σ_{v} was determined by fitting the predictions to the N-body simulations, using the data below the wavenumber indicated by the vertical arrow. The best-fit values of σ_{v} are $\sigma_{\mathrm{v}} = 395\,\mathrm{km\,s^{-1}}$ and $285\,\mathrm{km\,s^{-1}}$, with and without the A and B terms, respectively.

III. MODEL AND ASSUMPTIONS

Given the formulae for Fisher matrix analysis, we now move to the discussion on the parameter forecast study using the multipole power spectra, and compare the results with those obtained from the full 2D spectrum. Before doing this, in this section, we briefly describe the model and assumptions for redshift-space power spectrum relevant for spectroscopic measurement of BAOs.

In redshift space, clustering statistics generally suffer from the two competitive effects, i.e., enhancement and suppression of clustering amplitude, referred to as the Kaiser and Finger-of-God effects, respectively. While the Kaiser effect comes from the coherent motion of the mass (or galaxy), the Finger-of-God effect is mainly attributed to the virialized random motion of the mass residing at a halo. On weakly non-linear regime, a tight correlation between velocity and density fields still remains, and a mixture of Kaiser and Finger-of-God effects is expected to be significant. Thus, a careful treatment is needed for accurately modeling anisotropic power spectrum.

Recently, we have presented an improved prescription for matter power spectrum in redshift space taking account of both the non-linear clustering and redshift distortion [32]. Based on the perturbation theory calculation, the model can give an excellent agreement with results of N-body simulations, and a percent level precision is almost achieved over the scales of our interest on BAOs. The full 2D power spectrum of this model is very similar to the one proposed by Ref. [37], but includes the corrections:

$$P(k,\mu) = e^{-(k\mu\, f\sigma_{\mathrm{v}})^2}\Big\{P_{\delta\delta}(k) + 2\,f\,\mu^2\,P_{\delta\theta}(k) + f^2\,\mu^4\,P_{\theta\theta}(k) + A(k,\mu;f) + B(k,\mu;f)\Big\} \quad (14)$$

with the quantity f being the growth-rate parameter. Here, the power spectra $P_{\delta\delta}$, $P_{\theta\theta}$ and $P_{\delta\theta}$ denote the auto power spectra of density and velocity divergence, and their cross power spectrum, respectively. The velocity divergence θ is defined by $\theta \equiv -\nabla\boldsymbol{v}/(aHf)$. The quantity σ_{v} denotes the one-dimensional velocity dispersion[51], and the exponential prefactor characterizes the damping behavior by the Finger-of-God effect. For the purpose to model the shape and structure of BAOs in power spectrum, σ_{v} may be treated as a free parameter, and determine it by fitting the predictions to the observations.

A salient property of the model (14) is the presence of the terms A and B, which represent the higher-order couplings between velocity and density fields, usually neglected in the phenomenological models of redshift distortion. The explicit expressions for these terms are derived based on the standard treatment of perturbation theory, and the results are presented in Ref. [32]. A detailed investigation in our previous paper [32] reveals that the corrections A and B can give an important contribution to the acoustic structure of BAOs over the scales $k \sim 0.2h\mathrm{Mpc}^{-1}$, which give rise to a slight uplift in the amplitude of monopole and quadrupole spectra. With the improved treatment of the perturbation theory to compute $P_{\delta\delta}$, $P_{\theta\theta}$ and $P_{\delta\theta}$ (e.g., [35, 38]), the model (14) can give a better prediction than the existing models of redshift distortion. Fig. 1 plots the illustrated example showing that the model (14) reproduces the N-body results of monopole and quadrupole spectra quite well, and the precision of the agreement between prediction and simulation reaches a percent-level. Hence, in this paper, we adopt the model (14) as a fiducial model for matter power spectrum in redshift space.

Note that the model (14) generically produces the non-vanishing higher multipole spectra of $\ell > 4$, due to the damping factor, $e^{-(k\mu\, f\sigma_{\mathrm{v}})^2}$. Furthermore, the corrections A and B are expanded as power series of μ, which include the powers up to μ^6 for the A term, μ^8 for the B term. This indicates that the corrections additionally contribute to the higher multipoles, at least, up to $\ell = 8$. In this sense, the model (14) provides an interesting testing ground to estimate the extent to which the

useful cosmological information can be obtained from the lower-multipole spectra.

Then, assuming the linear galaxy bias in real space, $\delta_{\rm gal} = b\delta_{\rm mass}$, the redshift-space power spectrum for galaxies becomes

$$P_{\rm gal}(k,\mu) = e^{-(k\mu\, f\sigma_{\rm v})^2}\, b^2 \Big\{ P_{\delta\delta}(k) + 2\,\beta\,\mu^2\, P_{\delta\theta}(k) + \beta^2\,\mu^4\, P_{\theta\theta}(k) + b\, A(k,\mu;\beta) + b^2\, B(k,\mu;\beta) \Big\} \quad (15)$$

with $\beta = f/b$. The linear deterministic bias may be too simplistic assumption, and the effects of non-linearity and stochasticity in the galaxy bias might be non-negligible [39–41]. Our primary concern here is the qualitative aspects of the parameter estimation using the multipole spectra, based on a physically plausible model of redshift distortion. Since the galaxy bias itself does not produce additional clustering anisotropies, we simply adopt the linear bias relation for illustrative purpose.

Finally, notice that in addition to the clustering anisotropies caused by the peculiar velocity of galaxies, the observed galaxy power spectrum defined in comoving space further exhibits anisotropies induced by the Alcock-Paczynski effect. This is modeled as

$$P_{\rm obs}(k,\mu) = \frac{H(z)}{H_{\rm fid}(z)} \left\{ \frac{D_{A,\rm fid}(z)}{D_A(z)} \right\}^2 P_{\rm gal}(q,\nu), \quad (16)$$

where the quantity $P_{\rm gal}(q,\nu)$ at the right-hand-side represents the template for the redshift-space power spectrum in the absence of cosmological distortion, i.e., Eq.(15). The comoving wavenumber k and the directional cosine μ measured with the underlying cosmological model are related to the true ones q and ν by the Alcock-Paczynski effect through (e.g., [8, 42, 43])

$$q = k \left[\left(\frac{D_{A,\rm fid}}{D_A} \right)^2 + \left\{ \left(\frac{H}{H_{\rm fid}} \right) - \left(\frac{D_{A,\rm fid}}{D_A} \right)^2 \right\} \mu^2 \right]^{1/2}, \quad (17)$$

$$\nu = \left(\frac{H}{H_{\rm fid}} \right) \mu \times \left[\left(\frac{D_{A,\rm fid}}{D_A} \right)^2 + \left\{ \left(\frac{H}{H_{\rm fid}} \right) - \left(\frac{D_{A,\rm fid}}{D_A} \right)^2 \right\} \mu^2 \right]^{-1/2}, \quad (18)$$

The quantities $D_{A,\rm fid}$ and $H_{\rm fid}$ are the fiducial values of the angular diameter distance and Hubble parameter at a given redshift slice.

IV. RESULTS

In what follows, for illustrative purpose, we consider the hypothetical galaxy survey of the volume $V_s = 4h^{-3}{\rm Gpc}^3$ at $z = 1$, and examine how well we can constrain the distance information and growth-rate parameter, D_A, H, and f, from the low-multipole power spectra. We set the number density of galaxies, linear bias parameter and velocity dispersion to $\overline{n} = 5\times10^{-4}h^3{\rm Mpc}^{-3}$, $b = 2$ and $\sigma_{\rm v} = 395{\rm km\ s}^{-1}$. These values are used in the Fisher analysis as a canonical setup, but we also examine the variants of these parameter set to study the sensitivity of the forecast results. Note that the depth and the volume of the survey considered here roughly match those of a stage III class survey defined by the Dark Energy Task Force (DETF) [44].

To compute the Fisher matrix adopting the model of redshift-space power spectrum, Eq. (15), we just follow the procedure in Ref. [32] to calculate the redshift-space power spectra. That is, we use the improved PT developed by Ref. [35, 45] to account for a dominant contribution of the non-linear gravity to the power spectra $P_{\delta\delta}$, $P_{\delta\theta}$ and $P_{\theta\theta}$, and to adopt standard PT for small but non-negligible corrections of A and B terms. Detailed comparison with N-body simulations [32, 35] showed that this treatment can work well, and in our fiducial set of cosmological parameters, the model can give a percent-level precision at least up to the wavenumber $k \le 0.2h{\rm Mpc}^{-1}$ at $z = 1$.

Number of free parameters in the subsequent Fisher analysis is five in total, i.e., D_A, H, and f, in addition to the parameters b and $\sigma_{\rm v}$. Other cosmological parameters such as $\Omega_{\rm m}$ or $\Omega_{\rm b}$ are kept fixed. We assume that the cosmological model dependence of the power spectrum shape is perfectly known a priori from the precision CMB measurement by PLANCK [46]. The influence of the uncertainty in the power spectrum shape is discussed in Sec. IV C 2 in detail.

A. Two-dimensional errors

As a pedagogical example, let us first examine how the lower-multipole spectra can constrain the parameters D_A, H, and f. Fig. 2 shows the two-dimensional contour of the 1-σ (68% C.L.) errors on (D_A, H) (bottom-left), (D_A, f) (top-left), and (f, H)-planes (bottom right). Here, the Fisher matrix is computed adopting the model of redshift-space power spectrum (15) up to $k_{\rm max} = 0.2h{\rm Mpc}^{-1}$.

The magenta solid and cyan dashed lines respectively represent the constraints coming from the monopole (P_0) and quadrupole (P_2) power spectrum alone. As anticipated, only the single multipole spectrum cannot provide useful information to simultaneously constrain D_A, H, and f. In particular, for the constraints on D_A and H, there appear strong degeneracies, and the error ellipses are much elongated and inclined. These behaviors are basically deduced from the Alcock & Paczynski effect, and are consistent with the facts that the monopole spectrum is rather sensitive to the combination (D_A^2/H), while the quadrupole spectrum is sensitive to $(D_A\, H)$ (e.g., [8]). On the other hand, combining monopole and quadrupole greatly improves the constraints (indicated by blue, outer shaded region) not only on D_A and

H, but also on growth-rate parameter f. This is because the degeneracies between the parameters D_A and H constrained by the monopole differ from that by the quadrupole, and thus the combination of these two spectra leads to a substantial reduction of the size of error ellipses. Further, the growth-rate parameter is proportional to the strength of redshift distortion, and can be determined by the quadrupole-to-monopole ratio. Although the measurement of the galaxy power spectrum alone merely gives a constraint on $\beta = f/b$, provided the accurate CMB measurement for power spectrum normalization, we can separately determine the growth-rate parameter. Note that the combination of monopole and hexadecapole spectra also provides a way to determine the growth-rate parameter (red shaded region), although the error on f is a bit larger due to the small amplitude of hexadecapole spectrum.

For comparison, Fig. 2 shows the forecast constraints obtained from the full 2D power spectrum (green, inner shaded region). Further, we plot the results combining the monopole and quadrupole spectra, but neglecting the covariance between $\ell = 0$ and $\ell = 2$, i.e., $\widetilde{\mathrm{Cov}}^{02} = \widetilde{\mathrm{Cov}}^{20} = 0$ (blue, dotted lines). Clearly, using a full 2D shape of the redshift-space power spectrum leads to a tighter constraint, and the area of the two-dimensional error is reduced by a factor of $1.6 - 18$, compared with the constraints from the monopole and quadrupole spectra. The results indicate that the contribution of the higher multipoles is very important, and the additional information from quadrupole and hexadecapole spectra, each of which puts a different parameter degeneracy, seems to play a dominant role in improving the constraints. On the other hand, for joint constraints from the monopole and quadrupole, a role of the covariance $\widetilde{\mathrm{Cov}}^{02}$ or $\widetilde{\mathrm{Cov}}^{20}$ seems less important, and one may naively treat monopole and quadrupole power spectra as statistically independent quantities. However, these results are partially due to the properties of the galaxy samples characterized by several parameters, and may be altered in different assumptions or survey setup. This point will be investigated in some details in next subsection.

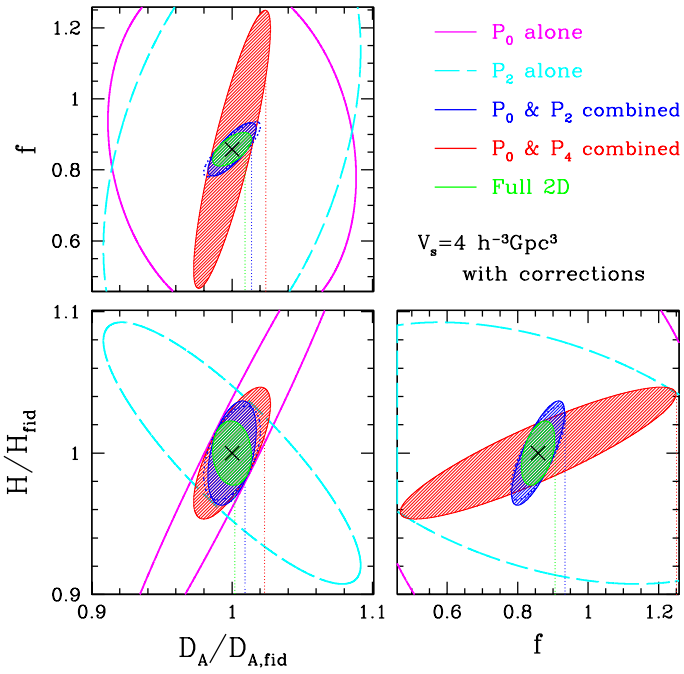

FIG. 2: Two dimensional contours of 1-σ (68%CL) errors on (D_A, H) (bottom-left), (D_A, f) (top-left), and (f, H) (bottom-right), assuming a stage-III class survey with $V_s = 4h^{-3}\mathrm{Gpc}^3$ at $z = 1$. In each panel, magenta solid and cyan dashed lines respectively indicate the forecast constraints coming from the monopole (P_0) and quadrupole (P_2) spectrum alone, while the blue and red shaded region represent the combined constraints from P_0 and P_2, and P_0 and P_4, respectively. The inner green shaded region is the results coming from the full 2D spectrum. As a reference, blue dotted contours show the results combining both P_0 and P_2, but (incorrectly) neglecting the covariance between monopole and quadrupole spectra, i.e., $\widetilde{\mathrm{Cov}}^{02} = \widetilde{\mathrm{Cov}}^{20} = 0$.

B. Figure-of-Merit

We here study the dependence of galaxy samples or survey setup on the forecast results for parameter constraints. To do this, it is useful to define the Figure-of-Merit (FoM):

$$\mathrm{FoM} \equiv \frac{1}{\sqrt{\det \widetilde{\boldsymbol{F}}^{-1}}}, \tag{19}$$

where the matrix $\widetilde{\boldsymbol{F}}^{-1}$ is the 3×3 sub-matrix, whose elements are taken from the inverse Fisher matrix $\boldsymbol{F}^{-1}$ associated with the parameters D_A, H, and f. The FoM quantifies the improvement of the parameter constraints, and inversely proportional to the product of one-dimensional marginalized errors, i.e., $\mathrm{FoM} \propto 1/\{\sigma(D_A)\sigma(H)\sigma(f)\}$.

Fig. 3 shows the dependence of FoM on the properties of the galaxy samples characterized by the number density $n_{\rm g}$ (top-right), bias parameter b (bottom-left), and one-dimensional velocity dispersion $\sigma_{\rm v}$ (bottom-right). Also, in top-left panel, we show the FoM as a function of maximum wavenumber $k_{\rm max}$ used in the parameter estimation study. Note that in plotting the results, the other parameters are kept fixed to the canonical values. The upper part of each panel plots the three different lines, and shows how the FoM changes depending on the choice or combination of power spectra used in the analysis: combining monopole (P_0) and quadrupole (P_2) spectra (magenta, dot-dashed); combining three multipole spectra, P_0, P_2 and P_4 (blue, long-dashed); using full 2D spectrum $P(k, \mu)$ (black, solid). On the other hand, the lower part of each panel plot the ratio of FoM normalized by the one for the full 2D spectrum.

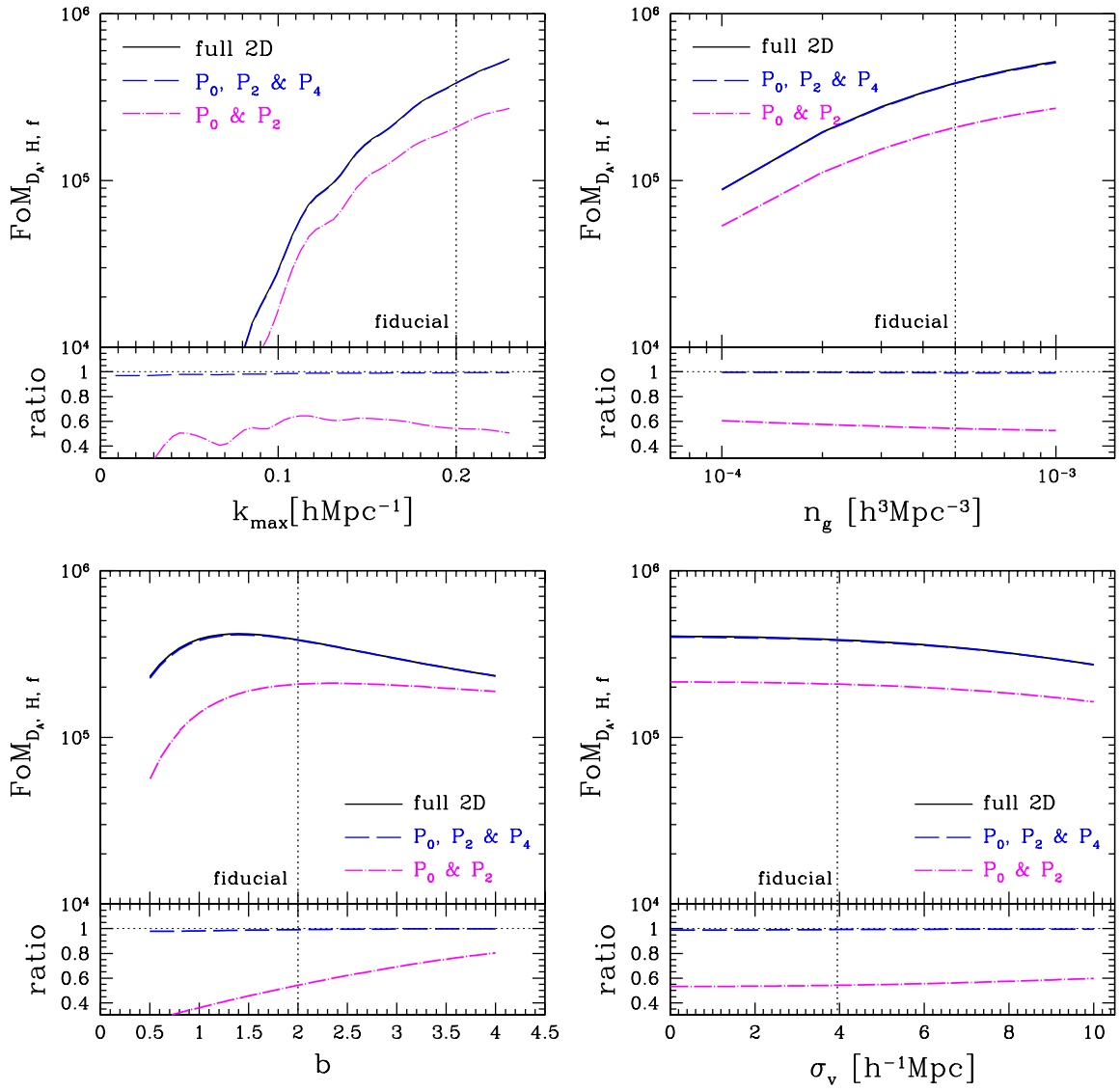

FIG. 3: Figure-of-merit (FoM) on the parameters D_A, H, and f defined by Eq. (19), as functions of $k_{\rm max}$ (top-left), $\overline{n}_{\rm gal}$ (top-right), b (bottom left), and $\sigma_{\rm v}$ (bottom right), assuming a hypothetical galaxy survey at $z = 1$ with volume $V_s = 4\,h^{-3}{\rm Gpc}^3$. In each panel, solid lines are the results obtained from the full 2D power spectrum, while the dashed and dot-dashed lines represent the FoM from the combination of the multipole spectra (dot-dashed: P_0 & P_2, dashed: P_0, P_0, & P_4). The bottom panels show the ratio of FoM normalized by the one obtained from the full 2D spectrum. Note that except the parameter along the horizontal axis, the fiducial values of the model parameters are set to $k_{\rm max} = 0.2\,h{\rm Mpc}^{-1}$, $n_{\rm g} = 5\times10^{-4}\,h^3{\rm Mpc}^{-3}$, $b = 2$, and $\sigma_{\rm v} = 3.95\,h^{-1}{\rm Mpc}$, indicated by the vertical dotted lines.

In principle, using the full 2D spectrum gives the tightest constraints on D_A, H, and f, but an interesting point here is that almost equivalent FoM to the one for the full 2D spectrum is obtained even from a partial information with the lower-multipole spectra P_0, P_2 and P_4. This is irrespective of the choice of the parameters for galaxy samples. Although the result may rely on the model of redshift distortion adopted in this paper, recalling the fact that the non-vanishing multipole spectra higher than $\ell \gtrsim 6$ arise only from the non-linear effects through the gravitational evolution and redshift distortion, the cosmological model dependence encoded in these higher multipoles is expected to be very weak, partly due to the low signal-to-noise ratio. In this sense, the result in Fig. 3 seems reasonable.

Now, turn to focus on the FoM from the combination of P_0 and P_2. Fig. 3 indicates that except for the case varying the bias b, the resultant FoM shows a monotonic dependence on the parameters. As a result, the ratio of FoM shown in the lower part of the panels is nearly constant around $0.4 - 0.6$. As for the variation of bias parameter, the non-monotonic dependence of the

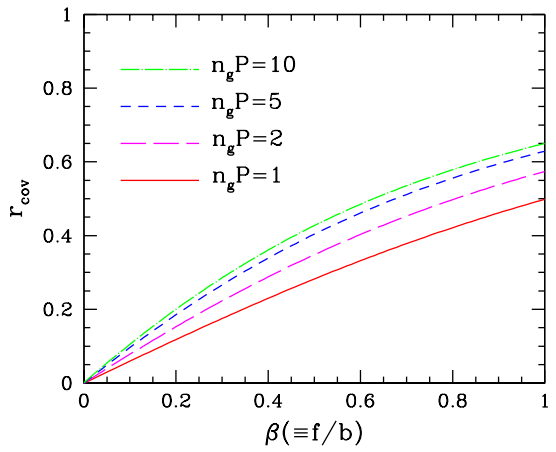

FIG. 4: Correlation coefficient for the covariance, $r_{\rm cov} = \widetilde{\rm Cov}^{0,2}/[\widetilde{\rm Cov}^{0,0}\widetilde{\rm Cov}^{2,2}]^{1/2}$, as function of $\beta \equiv f/b$. The plotted results are obtained based on the linear theory, in which the coefficient $r_{\rm cov}$ depends on the power spectrum amplitude relative to the shot-noise contribution, $n_{\rm g}\,P$, as well as β. The solid, long-dashed, short-dashed, and dot-dashed lines respectively indicate the results with $n_{\rm g}\,P = 1$, 2, 5, and 10.

FoM is basically explained by the two competitive effects. That is, as increasing b, while the power spectrum amplitude increases and signal-to-noise ratio is enhanced, the clustering anisotropies due to the redshift distortion controlled by the quantity β are gradually reduced. Hence, for some values of b, FoM becomes maximum. A noticeable point is that the ratio of FoM for the monopole and quadrupole becomes gradually increased as the clustering bias becomes large. At $b \sim 4$, the ratio of FoM reaches at 0.8, indicating most of the cosmological information contained in the hexadecapole and higher multipoles is lost, and signals coming from the monopole and quadrupole spectra becomes dominated.

The reason for this behavior is presumably due to the covariance between the multipole spectra, $\widetilde{\rm Cov}^{\ell\ell'}$. In linear regime, the covariance neglecting the shot noise contribution is determined by the galaxy power spectrum in real space and parameter $\beta = f/b$, and the off-diagonal component $\widetilde{\rm Cov}^{02} = \widetilde{\rm Cov}^{20}$ is roughly proportional to β. Thus, as increasing the clustering bias b while keeping the growth-rate parameter, the covariance $\widetilde{\rm Cov}^{02}$ becomes smaller, and the monopole and quadrupole power spectra become statistically independent. To see this more explicitly, we define

$$r_{\rm cov} = \frac{\widetilde{\rm Cov}^{0,2}}{[\widetilde{\rm Cov}^{0,0}\widetilde{\rm Cov}^{2,2}]^{1/2}}. \tag{20}$$

In Fig. 4, taking account of the shot noise contribution, the quantity $r_{\rm cov}$ is plotted against the parameter β. Here, we used the linear theory to calculate $\widetilde{\rm Cov}^{\ell\ell'}$. Fig. 4 implies that in our fiducial setup with $f = 0.858$, $r_{\rm cov}$ becomes $\lesssim 0.2$ for the bias $b = 4$. Since the smaller values of β also suppress the Kaiser effect in the covariances $\widetilde{\rm Cov}^{00}$ and $\widetilde{\rm Cov}^{22}$, the constraints from the monopole and quadrupole spectra is relatively improved.

The result suggests that even the partial information with monopole and quadrupole spectra still provides a fruitful constraint on D_A, H and f, depending on the survey setup. In this respect, a benefit to use these power spectra should be further explored. As a next step, we will discuss the robustness of the parameter constraints against the systematic biases.

C. Impact of systematic biases

Among various envisaged systematics that affect the parameter constraints, the incorrect assumption for the theoretical template of power spectra may seriously lead to a bias in the best-fit parameters. There are several routes to produce an incorrect theoretical template; incorrect model of redshift distortion and/or non-linear gravitational evolution, wrong prior information for cosmological parameters, and improper parametrization for galaxy bias. In this subsection, we specifically examine the first and second cases. We first discuss the incorrect model of redshift distortion, and quantify the size of the systematic bias in the best-fit parameter. The influence of the wrong prior information will be discussed in next subsection.

1. *Systematic biases from a wrong model of redshift distortion*

Let us first discuss the impact of incorrect model of redshift distortion on the parameter estimation. To be precise, we consider the small discrepancy in the theoretical template for redshift-space power spectrum (15), and estimate the systematic biases from Eq.(11). Fig. 5 shows the systematic biases caused by the incorrect model template neglecting the A and B terms. We plot the results by varying the model parameters, $k_{\rm max}$ (top-left), $n_{\rm g}$ (top-right), b (bottom-left), and $\sigma_{\rm v}$ (bottom-right), around the fiducial values. In each panel, the first three panels from the top plot the deviation of the best-fit value from the fiducial one, δf, δD_A, and δH, normalized by their fiducial values. On the other hand, the lowest panel shows the Figure-of-Bias (FoB), which represents the statistical significance of systematic biases relative to the statistical errors, defined by [47, 48]:

$$\mathrm{FoB} \equiv \left(\sum_{i,j} \delta\theta_i \widetilde{\boldsymbol{F}'}_{ij} \delta\theta_j \right)^{1/2} \tag{21}$$

Note that the matrix $\widetilde{\boldsymbol{F}'}_{ij}$ is the same inverse of the submatrix $\widetilde{\boldsymbol{F}}_{ij}^{-1}$ as defined in Eq. (19), but with the Fisher

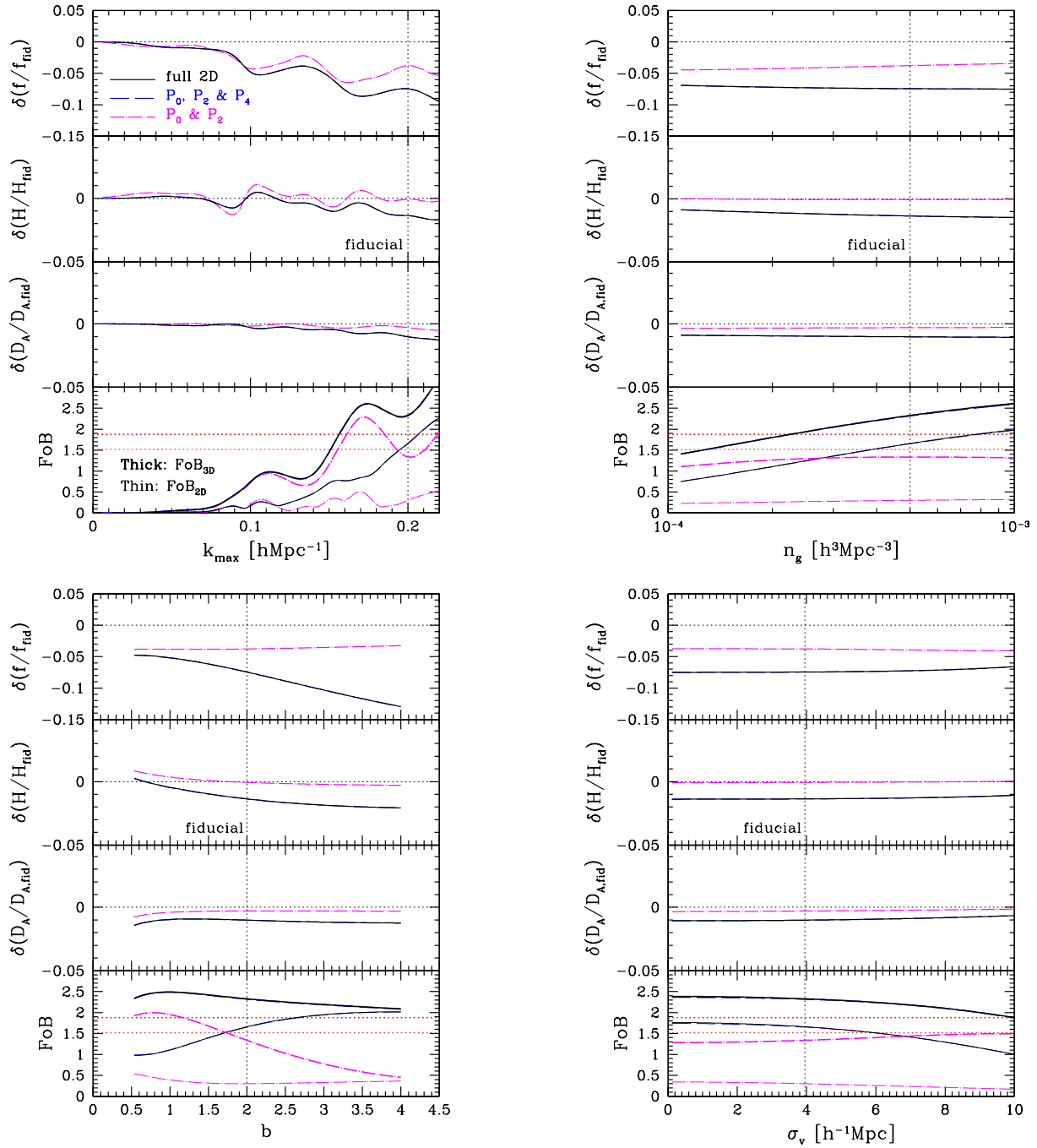

FIG. 5: Systematic biases for best-fit values of parameters f, D_A and H and Figure-of-Bias as function of $k_{\rm max}$ (top-left), $n_{\rm g}$ (top-right), b (bottom-left), and $\sigma_{\rm v}$ (bottom-right). These are the estimates adopting the 'incorrect' model of redshift-space power spectrum, in which we ignore the small correction terms, A and B. In bottom panels of each figure, thick and thin lines respectively show the FoB in three and two-dimensions, i.e., (D_A, H, f) and (D_A, H). The dotted lines indicates the 1-σ significance of the deviation relative to the statistical error. Note that the shift of the best-fit parameters remains unchanged irrespective of the survey volume V_s, while the FoB given here represents the specific results with the survey volume $V_s = 4h^{-3}{\rm Gpc}^3$. The fiducial values of the model parameters used in the calculation are the same as in Fig. 3 (indicated by vertical dotted lines), except the parameter along the horizontal axis.

matrix obtained from the incorrect template. With the above definition, the FoB squared simply reflects the $\Delta\chi^2$ for the true values of the parameters relative to the biased estimate of the best-fit values [48]. Thus, in the cases with three parameters, if the FoB exceeds 1.88 (indicated by the red, thick dotted lines), the true values of the parameters would go outside the 1-σ (68%C.L.) error ellipsoid of the biased confidence region. Notice that the shift of best-fit parameters remains unchanged irrespective of the survey volume V_s, while the FoB is

proportional to $V_s^{1/2}$.

Fig. 5 shows that the biases in the distance information, δD_A and δH, are basically small and reach $1-2\%$ at most, but the bias in the growth-rate parameter, δf, is rather large. Hence, the behaviors of the FoBs indicated by the thick lines are mostly dominated by the error and bias in the growth-rate parameter. As a result, for some ranges of parameters, the expected FoB using a full-shape information (black solid, labeled as 'full 2D') tends to exceed the critical value, 1.88. This is true even if we marginalize over f and just focus on the distance information D_A and H, depicted as thin lines in the lowest panels (labeled as '$\mathrm{FoB_{2D}}$'). Note that in the case of two parameters, the true values of D_A and H are ruled out at 1-σ level if FoB exceeds 1.52 (red, thin dotted lines).

On the other hand, if we use the information obtained only from the monopole and quadrupole spectra (magenta, dot-dashed lines), the systematic biases are significantly reduced, and the resultant FoBs are well within the critical values except for unrealistic case with a large $\sigma_{\rm v}$ or anti-bias $b \lesssim 1$. If we are just interested in D_A and H marginalized over f, the FoB becomes substantially smaller, and would be far below the critical value 1.52, even for a large galaxy survey with $V_s \lesssim 40h^{-3}\mathrm{Mpc}^3$. Therefore even the partial information from the monopole and quadrupole spectra is helpful and rather robust against the systematic biases than the full 2D information. Although the figure-of-merit for the constraints on D_A, H and f would be degraded, the reduction of FoM is at most factor of ~ 0.6, which can be improved to ~ 0.8 for highly biased objects (see Fig. 3).

Finally, there are several interesting points to be noted. One is the oscillatory behavior of the systematic biases and FoB shown in the top-left panel. This is originated from the acoustic structure of the power spectrum, and the result suggests that the bias in the growth-rate parameter δf is sensitively affected by the BAO measurement. Another noticeable feature is a suppression of the FoB in the case of three parameters using the monopole and quadrupole spectra, which appears at a larger value of the galaxy bias b (thick, dot-dashed line in bottom-left panel). This is presumably due to the multiple effects that as increasing the clustering bias, the systematic bias for the growth-rate parameter tends to be slightly reduced, while the constraint on the growth-rate parameter becomes gradually weaker. There also appears a similar trend in the case using a full 2D spectrum, but the suppression is rather small and FoB never falls below the critical value, 1.88. This is because the biased estimate of growth-rate parameter, δf, significantly deviates from the fiducial value, as opposed to the case using monopole and quadrupole spectra.

2. *Systematic biases from incorrect prior information*

So far, we have assumed that the underlying cosmological parameters necessary to compute the redshift-space power spectrum are whole known a priori from the CMB observations such as PLANCK. However, even the precision CMB measurement produces some uncertainties in the cosmological parameters due to the parameter degeneracy. This may give an important source for the incorrect theoretical template for redshift-space power spectrum, and leads to a biased estimate of D_A, H, and f.

Fig. 6 quantifies the size of systematic biases and FoB arising from the incorrect assumptions for cosmological parameters. Here, we especially focus on the parameters A_s, $\Omega_{\rm m}$, and h fixing $\Omega_{\rm m}h^2$ constant, and plot the sensitivity of the systematic biases to the variation of those parameters. Note that in computing the power spectrum, we strictly assume the flat cosmological model and the model of redshift distortion (15) as a fiducial model of power spectrum template.

Compared to the results in Sec. IV C 1, the systematic bias in the growth-rate parameter is relatively small, and the significance of the biases in the acoustic-scale information conversely increases. That is, the best-fit values of the parameters D_A and H is rather sensitive to the precision of the prior information in the power spectrum template. A noticeable point is that this is true irrespective of the choice of the template power spectra used in the parameter estimation (i.e., full 2D spectrum or combination of P_0 and P_2). As a result, a percent-level precision is generally required for the prior information of cosmological parameters, except for the scalar spectral amplitude, A_s. Through the non-linear clustering and/or redshift distortion, a small change in A_s alters the power spectrum shape, and it can potentially affect the acoustic scale and the clustering anisotropies. However, at $z=1$, the non-linear effects on the scales of our interest, $k \lesssim 0.2h\mathrm{Mpc}^{-1}$, is rather mild, and the resultant impact on the acoustic-scale measurement is extremely small. Hence, for a typical survey volume of stage III-class survey with $V_s \sim 4h^{-3}\mathrm{Gpc}^3$, no appreciable systematic bias might be produced from the incorrect prior assumption on A_s.

V. SUMMARY

In this paper, we have studied the cosmological constraints from the anisotropic BAOs based on the multipole expansion of redshift-space power spectrum. We have derived the several formulae for the Fisher analysis using the multipole power spectra; Eqs. (7) and (8) for the Fisher matrix, and Eqs. (11) and (12) for the estimation of systematic biases. We then consider the hypothetical galaxy survey of $V_s = 4h^{-3}\mathrm{Gpc}^3$ and $z=1$, and discuss the potential power of the lower multipole spectra on the cosmological constraints, particularly focusing on the parameters D_A, H and f.

Compared to the analysis with full 2D power spectrum, a partial information from the monopole and quadrupole power spectra generally degrades the constraints on D_A, H, and f. Typically, the constraint is degraded by a fac-

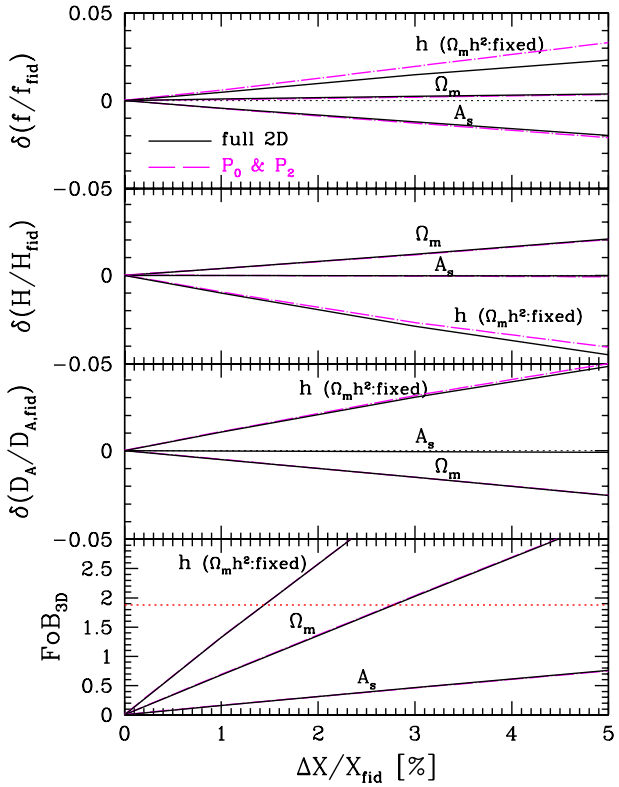

FIG. 6: Systematic biases for the best-fit values of the parameters f, D_A and H, and FoB for these three parameters (from top to bottom), adopting the incorrect prior information for cosmological parameters in computing the template power spectrum; $X = A_s$, $\Omega_{\rm m}$, and h ($\Omega_{\rm m}h^2$: fixed). The results are plotted against the fractional difference between the correct and incorrect values of each cosmological parameters, $\Delta X/X_{\rm fid}$. Solid and dashed lines represent the results from a full 2D power spectrum and partial information with monopole and quadrupole spectra, respectively. Note that in bottom panel, the horizontal dotted lines indicates the 1-σ significance of the deviation relative to the statistical error.

tor of ~ 1.3 for each parameter. The interesting finding is that adding the information from hexadecapole spectra (P_4) to that from the monopole and quadrupole spectra greatly improves the constraints, and the resultant constraints would become almost comparable to those expected from the full 2D power spectrum (see Fig. 3). Note also that the situation would be relatively improved depending on the properties of galaxy samples, and for highly biased galaxy samples with $b \sim 4$, the total power of the constraints defined by the Figure-of-Merit [FoM, Eq. (19)] can reach $\sim 80\%$ of the one expected from the full 2D power spectrum.

We have also investigated the impacts of systematic biases on the best-fit values of D_A, H and f. The incorrect model of redshift distortion tends to produce a large systematic bias in the growth-rate parameter, and the size of biases would be rather significant for the analysis with full 2D spectrum. An interesting suggestion is that the situation would be greatly relaxed if we only use the combination of monopole and quadrupole spectra, and the estimated value of Figure-of-Bias defined by Eq. (21) is mostly below the critical value for stage-III class surveys (Fig. 5). In this respect, the analysis with partial information from monopole and quadrupole may be still helpful in cross-checking the results derived from the full 2D power spectrum. On the other hand, wrong prior assumption of cosmological parameters in computing the template power spectrum severely affects the acoustic-scale determination, and a percent-level precision is required for the prior information in order to avoid a large systematic biases on D_A and H (Fig. 6). This is true irrespective of the choice of template power spectra used in the analysis.

Finally, we note that the assumptions and situations considered in the paper are somewhat optimistic or too simplistic, and a more careful study is needed for a quantitative parameter forecast. One critical aspect is the modeling of the galaxy power spectrum. In reality, the assumption of linear and deterministic galaxy biasing is idealistic, and the scale-dependence or non-linearity/stochasticity of the galaxy biasing should be consistently incorporated into the theoretical template of redshift-space power spectrum. Although this is tiny effect for the scale of our interest, the distance information, D_A and H, is rather sensitive to a slight modification of the acoustic structure in the power spectrum, and results in this paper might be somehow changed. A more elaborate modeling for power spectrum is thus quite essential.

Acknowledgments

AT is supported by a Grant-in-Aid for Scientific Research from the Japan Society for the Promotion of Science (JSPS) (No. 21740168). TN is supported by JSPS. SS is supported by JSPS through research fellowships and Excellent Young Researchers Overseas Visit Program (No.21-00784). This work was supported in part by Grant-in-Aid for Scientific Research on Priority Areas No. 467 "Probing the Dark Energy through an Extremely Wide and Deep Survey with Subaru Telescope", JSPS Core-to-Core Program "International Research Network for Dark Energy", and World Premier International Research Center Initiative (WPI Initiative), MEXT, Japan.

[1] D. J. Eisenstein et al. (SDSS), Astrophys. J. **633**, 560 (2005), astro-ph/0501171.
[2] W. J. Percival et al., Mon. Not. Roy. Astron. Soc. **381**, 1053 (2007), 0705.3323.
[3] W. J. Percival et al., Mon. Not. Roy. Astron. Soc. **401**, 2148 (2010), 0907.1660.
[4] C. Alcock and B. Paczynski, Nature **281**, 358359 (1979).
[5] H.-J. Seo and D. J. Eisenstein, Astrophys. J. **598**, 720 (2003), astro-ph/0307460.
[6] C. Blake and K. Glazebrook, Astrophys. J. **594**, 665 (2003), astro-ph/0301632.
[7] M. Shoji, D. Jeong, and E. Komatsu, Astrophys. J. **693**, 1404 (2009), 0805.4238.
[8] N. Padmanabhan and M. J. White, 1, Phys. Rev. **D77**, 123540 (2008), 0804.0799.
[9] E. V. Linder, Astropart. Phys. **29**, 336 (2008), 0709.1113.
[10] L. Guzzo et al., Nature **451**, 541 (2008), 0802.1944.
[11] K. Yamamoto, T. Sato, and G. Huetsi, Prog. Theor. Phys. **120**, 609 (2008), 0805.4789.
[12] Y.-S. Song and W. J. Percival, JCAP **0910**, 004 (2009), 0807.0810.
[13] D. Schlegel, M. White, and D. Eisenstein (with input from the SDSS-III) (2009), 0902.4680.
[14] G. J. Hill et al. (2008), 0806.0183.
[15] J. P. Beaulieu et al. (2010), 1001.3349.
[16] N. Gehrels (2010), 1008.4936.
[17] H.-J. Seo and D. J. Eisenstein, Astrophys. J. **665**, 14 (2007), astro-ph/0701079.
[18] M. White, Y.-S. Song, and W. J. Percival, Mon. Not. Roy. Astron. Soc. **397**, 1348 (2008), 0810.1518.
[19] T. Okumura et al., Astrophys. J. **676**, 889 (2008), 0711.3640.
[20] R. Takahashi et al., Astrophys. J. **700**, 479 (2009), 0902.0371.
[21] A. Cabre and E. Gaztanaga, Mon. Not. Roy. Astron. Soc. **393**, 1183 (2009), 0807.2460.
[22] N. Kaiser, Mon. Not. Roy. Astron. Soc. **227**, 1 (1987).
[23] A. J. S. Hamilton, Astrophys. J. **385**, L5 (1992).
[24] A. J. S. Hamilton (1997), astro-ph/9708102.
[25] D. Tocchini-Valentini, M. Barnard, C. L. Bennett, and A. S. Szalay (2011), 1101.2608.
[26] E. Komatsu et al. (WMAP), Astrophys. J. Suppl. **180**, 330 (2009), 0803.0547.
[27] K. Yamamoto, Astrophys. J. **595**, 577 (2003), astro-ph/0208139.
[28] M. Tegmark, Phys. Rev. Lett. **79**, 3806 (1997), astro-ph/9706198.
[29] H. A. Feldman, N. Kaiser, and J. A. Peacock, Astrophys. J. **426**, 23 (1994), astro-ph/9304022.
[30] K. Yamamoto, M. Nakamichi, A. Kamino, B. A. Bassett, and H. Nishioka, Publ. Astron. Soc. Jap. **58**, 93 (2006), astro-ph/0505115.
[31] S. Saito, M. Takada, and A. Taruya, Phys. Rev. **D80**, 083528 (2009), 0907.2922.
[32] A. Taruya, T. Nishimichi, and S. Saito (2010), 1006.0699.
[33] R. Takahashi et al. (2009), 0912.1381.
[34] M. C. Neyrinck and I. Szapudi (2007), 0710.3586.
[35] A. Taruya, T. Nishimichi, S. Saito, and T. Hiramatsu, Phys. Rev. **D80**, 123503 (2009), 0906.0507.
[36] D. J. Eisenstein and W. Hu, Astrophys. J. **496**, 605 (1998), astro-ph/9709112.
[37] R. Scoccimarro, Phys. Rev. **D70**, 083007 (2004), astro-ph/0407214.
[38] M. Crocce and R. Scoccimarro, Phys. Rev. **D77**, 023533 (2008), 0704.2783.
[39] T. Okumura and Y. P. Jing, Astrophys. J. **726**, 5 (2011), 1004.3548.
[40] D. Jeong and E. Komatsu, Astrophys. J. **691**, 569 (2009), 0805.2632.
[41] S. Saito, M. Takada, and A. Taruya (2010), 1006.4845.
[42] W. E. Ballinger, J. A. Peacock, and A. F. Heavens, Mon. Not. Roy. Astron. Soc. **282**, 877 (1996), astro-ph/9605017.
[43] H. Magira, Y. P. Jing, and Y. Suto, Astrophys. J. **528**, 30 (2000), astro-ph/9907438.
[44] A. J. Albrecht et al. (2006), astro-ph/0609591.
[45] A. Taruya and T. Hiramatsu, Astrophys.J. **674**, 617 (2008), 0708.1367.
[46] (2006), astro-ph/0604069.
[47] S. Joudaki, A. Cooray, and D. E. Holz, Phys. Rev. D **80**, 023003 (2009), 0904.4697.
[48] C. Shapiro, Astrophys. J. **696**, 775 (2009), 0812.0769.
[49] Throughout the paper, we work with the distant-observer approximation, and neglect the angular dependence of the line-of-sight direction, relevant for the high-redshift galaxy surveys.
[50] Here, we use the standard notation for the multipole expansion of redshift power spectra given by (1), which differs from the definition of Ref. [30]
[51] The definition of velocity dispersion $\sigma_{\rm v}$ adopted in this paper differs from the one commonly used in the literature by a factor of f, but coincides with those in Refs. [32, 37].